Inscribing and separating an ellipsoid and a constrained zonotope: Applications in stochastic control and centering

Vinod, Abraham P.; Weiss, Avishai; Di Cairano, Stefano

TR2024-173 December 18, 2024

Abstract

Constrained zonotopes are equivalent representations for convex polytopes that have recently enabled tractable implementations of some set-based control methods. We con- sider the problems of inscribing an ellipsoid within and separating an ellipsoid from a constrained zonotope. Such problems arise in several applications, including in stochastic optimal control problems when enforcing chance constraints involving constrained zonotopes. Given a parameterized ellipsoid, we propose a set of sufficient conditions that are convex in the parameters and guarantee that the ellipsoid is inscribed within a constrained zonotope. We use these conditions to solve a two-stage, return-guaranteed spacecraft rendezvous problem under uncertainty. We also apply these conditions to tractably approximate the Chebyshev center and the maximum volume inscribed ellipsoid of a constrained zonotope using linear and second-order cone programming. We also propose a set of necessary and sufficient conditions that separate an ellipsoid from a constrained zonotope, which has applications in enforcing probabilistic exclusion from a constrained zonotope.

IEEE Conference on Decision and Control (CDC) 2024

Inscribing and separating an ellipsoid and a constrained zonotope: Applications in stochastic control and centering

Abraham P. Vinod*, Avishai Weiss, and Stefano Di Cairano

***Abstract*— Constrained zonotopes are equivalent representations for convex polytopes that have recently enabled tractable implementations of some set-based control methods. We consider the problems of inscribing an ellipsoid within and separating an ellipsoid from a constrained zonotope. Such problems arise in several applications, including in stochastic optimal control problems when enforcing chance constraints involving constrained zonotopes. Given a parameterized ellipsoid, we propose a set of sufficient conditions that are convex in the parameters and guarantee that the ellipsoid is inscribed within a constrained zonotope. We use these conditions to solve a two-stage, return-guaranteed spacecraft rendezvous problem under uncertainty. We also apply these conditions to tractably approximate the Chebyshev center and the maximum volume inscribed ellipsoid of a constrained zonotope using linear and second-order cone programming. We also propose a set of necessary and sufficient conditions that separate an ellipsoid from a constrained zonotope, which has applications in enforcing probabilistic exclusion from a constrained zonotope.**

I. INTRODUCTION

Constrained zonotopes describe convex polytopes exactly, and provide an alternative to the traditional halfspace/vertex representations [1]–[5]. They express a convex polytope as an affine transformation of a high-dimensional unit cube after intersecting the cube with a set of affine constraints. The main advantage of a constrained zonotope representation is that it admits closed-form expressions for several set operations relevant to set-based control [1]–[5]. For example, using the recent results on closed-form approximations of the Pontryagin difference involving constrained zonotopes [5], one can now efficiently compute robust controllable sets for high-dimensional systems over long horizons without requiring vertex-facet enumeration. On the other hand, there are still several open questions regarding the use of constrained zonotopes in optimal control, including efficient formulations for imposing chance constraints involving constrained zonotopes and computing the Chebyshev center of a constrained zonotope. This paper builds upon the recent results in [5] to *investigate problems arising from the interactions of constrained zonotopes and ellipsoids with applications in stochastic optimal control and computational geometry.*

We are motivated by the problem of designing *two-staged, return-guaranteed, spacecraft rendezvous* trajectories. Here, we seek rendezvous trajectories in the first stage that steer a control-constrained spacecraft towards a rendezvous target, while allowing for the possibility of diverting back to a holding position in the event of a no-go decision in the beginning of the second stage. This allows the rendezvous target to request the approaching spacecraft to abort rendezvous, if needed, and safely steer away from the docking area. The rendezvous trajectory in both stages must also account for process and measurement uncertainties arising from the actuation and sensing limitations [6]. We encode the desirable property of the approaching spacecraft being able to either return to a holding position or to continue towards the target for docking in the second stage using robust controllable sets, see, similar to [7], [8]. We use these sets to constrain the terminal state of the rendezvous trajectory in the first stage. Recall that polytope-based computation of robust controllable sets for high-dimensional systems suffer from numerical issues due to projection [9]–[11]. For non-stochastic, symmetric, convex, and compact disturbances, we can use constrained zonotopes to efficiently compute the required high-dimensional robust controllable sets [5]. However, under stochastic models for the uncertainty in the first stage, we need tractable approaches to enforce chance constraints involving constrained zonotopes.

The first part of this paper focuses on the problem of inscribing an ellipsoid within a constrained zonotope. We propose a collection of convex constraints to guarantee that an ellipsoid is inscribed in a constrained zonotope, which has several applications. These constraints enable us to conservatively enforce chance constraints using the well-known ellipsoidal approximation [12], [13]. Given a random vector $\boldsymbol{x}$, decision variable z, a constrained zonotope $\mathcal{C}$ and a threshold $\delta \in (0,1)$, $z + \mathcal{E}(\delta) \subseteq \mathcal{C} \Rightarrow \mathbb{P}\{\boldsymbol{x} + z \in \mathcal{C}\} \geq \delta$ for an appropriately defined ellipsoid $\mathcal{E}(\delta)$ [12, Sec. 3.1]. In addition, we can use these constraints to compute the Chebyshev center and the maximum volume inscribed ellipsoid of a constrained zonotope. Chebyshev centering problems have applications in optimization and model predictive control [11], [14]. The maximum volume inscribed ellipsoid provides a succinct approximation of constrained zonotopes that can be useful for analysis and visualization.

The second part of the paper focusses on separating a parameterized ellipsoid from a constrained zonotope. Such separation problems arise in collision-checking [13], [15] as well as when enforcing chance constraints of the form $\mathbb{P}\{\boldsymbol{x}+z \notin \mathcal{C}\} \geq \delta$. However, unlike the inscribed ellipsoid problem, these constraints are non-convex on the ellipsoid parameters.

The main contributions of this paper are as follows: 1) characterize necessary and sufficient conditions for an ellipsoid to be inscribed within a constrained zonotope, 2) characterize necessary and sufficient conditions for an ellipsoid to be separated from a constrained zonotope, and 3) exploit

*Corresponding author. Email: abraham.p.vinod@ieee.org
A. P. Vinod, A. Weiss, and S. Di Cairano are with Mitsubishi Electric Research Laboratories, Cambridge, MA 02139, USA.

the structure in these conditions to enable tractable formulations of chance constraints involving constrained zonotopes as well as (approximately) compute the maximum volume inscribed ellipsoid and the Chebyshev center of a constrained zonotope. We also use the proposed constraint formulations in combination with constrained zonotopic computation of robust controllable sets [5] to design a rendezvous trajectory for a two-stage spacecraft rendezvous problem.

II. Preliminaries

$0_{n\times m}$ and $1_{n\times m}$ are matrices of zeros and ones in $\mathbb{R}^{n\times m}$ respectively, $\mathbb{S}_n$ is the set of symmetric matrices in $\mathbb{R}^{n\times n}$, $\mathbb{L}_n$ is the set of lower-triangular matrices in $\mathbb{R}^{n\times n}$, I_n is the n-dimensional identity matrix, $\mathrm{diag}(d)$ is the n-dimensional diagonal matrix with entries from $d\in\mathbb{R}^n$, $\mathbb{N}_{[a:b]}$ is the subset of natural numbers between (and including) $a,b\in\mathbb{N}$, $a\leq b$, e_i is the standard axis vectors of $\mathbb{R}^n$, and $\|\cdot\|_p$ is the ℓ_p-norm of a vector. Let $M\in\mathbb{R}^{m\times n}$, $M_1\in\mathbb{R}^{m\times n_1}$, and $M_2\in\mathbb{R}^{m_1\times n}$. Then, $[M,M_1]\in\mathbb{R}^{m\times(n+n_1)}$ and $[M;M_2]\in\mathbb{R}^{(m+m_1)\times n}$ are matrices obtained by concatenating M and M_1 horizontally, and M and M_2 vertically respectively. For $M\in\mathbb{R}^{m\times n}$ with full row rank, $M^\dagger=M^\top\left(MM^\top\right)^{-1}$ denotes its (right) pseudoinverse, and $x=M^\dagger v$ solves the system of linear equation $Mx=v$ for any vector $v\in\mathbb{R}^m$.

For any set $\mathcal{S}\subseteq\mathbb{R}^n$, $\mathrm{AH}(\mathcal{S})$ is an affine set such that $\mathcal{S}\subseteq\mathcal{A}\Rightarrow\mathrm{AH}(\mathcal{S})\subseteq\mathcal{A}$ for any affine set $\mathcal{A}$. The *affine dimension* of a set $\mathcal{S}$ is the dimension of the subspace associated with $\mathrm{AH}(\mathcal{S})$. A *full-dimensional* set in $\mathbb{R}^n$ is a non-empty set with an affine dimension of n [14, Sec. 2.1].

From probability theory, for any events $\mathcal{A}$ and $\mathcal{B}$,

$$\mathbb{P}\{\mathcal{A}\}\geq\mathbb{P}\{\mathcal{A}\cap\mathcal{B}\}=\mathbb{P}\{\mathcal{A}|\mathcal{B}\}\mathbb{P}\{\mathcal{B}\},\tag{1a}$$
$$\mathcal{B}\subseteq\mathcal{A}\Longrightarrow\mathbb{P}\{\mathcal{A}|\mathcal{B}\}=1\text{ and }\mathbb{P}\{\mathcal{A}\}\geq\mathbb{P}\{\mathcal{B}\}.\tag{1b}$$

Here, $\mathcal{B}\subseteq\mathcal{A}$ denotes that the occurrence of the event $\mathcal{B}$ guarantees the occurrence of the event $\mathcal{A}$ almost surely.

A. Sets: Constrained zonotopes, polytopes, and ellipsoids

Let $\mathcal{P}$ and $\mathcal{C}$ be convex and compact sets in $\mathbb{R}^n$. Then, $\mathcal{P}$ is a (convex) *polytope* if (2a) holds and $\mathcal{C}$ is a *constrained zonotope* if (2b) holds:

$$\exists(H_P,k_P)\in\mathbb{R}^{N_P\times n}\times\mathbb{R}^{N_P}:\mathcal{P}=\{x:H_Px\leq k_P\},\tag{2a}$$
$$\exists(G_C,c_C,A_C,b_C)\in\mathbb{R}_C:\mathcal{C}=\left\{G_C\xi+c_C\,\middle|\,\begin{array}{c}\|\xi\|_\infty\leq 1,\\ A_C\xi=b_C\end{array}\right\},\tag{2b}$$

where $\mathbb{R}_C\triangleq\mathbb{R}^{n\times N_C}\times\mathbb{R}^n\times\mathbb{R}^{M_C\times N_C}\times\mathbb{R}^{M_C}$. From [1, Thm. 1], representations (2a) and (2b) are equivalent, with a tractable approach to convert (2a) to (2b). However, converting (2b) to (2a) is computationally expensive.

The main advantage of constrained zonotopes (2b) over polytopic representation (2a) is the closed-form expressions for several set operations. Specifically, for any sets $\mathcal{C},\mathcal{S}\subseteq\mathbb{R}^n$ and $\mathcal{W}\subseteq\mathbb{R}^m$, and a matrix $R\in\mathbb{R}^{m\times n}$, the set operations (affine map, Minkowski sum $\oplus$, intersection with inverse affine map $\cap_R$, and Pontryagin difference $\ominus$) are:

$$R\mathcal{C}\triangleq\{Ru:u\in\mathcal{C}\},\tag{3a}$$
$$\mathcal{C}\oplus\mathcal{S}\triangleq\{u+v:u\in\mathcal{C},\ v\in\mathcal{S}\},\tag{3b}$$
$$\mathcal{C}\cap_R\mathcal{W}\triangleq\{u\in\mathcal{C}:Ru\in\mathcal{W}\},\tag{3c}$$
$$\mathcal{C}\ominus\mathcal{S}\triangleq\{u:\forall v\in\mathcal{S},u+v\in\mathcal{C}\}.\tag{3d}$$

Since $\mathcal{C}\cap\mathcal{S}=\mathcal{C}\cap_{I_n}\mathcal{S}$, (3c) also includes the standard intersection. For any $x\in\mathbb{R}^n$, we use $\mathcal{C}+x$ and $\mathcal{C}-x$ to denote $\mathcal{C}\oplus\{x\}$ and $\mathcal{C}\oplus\{-x\}$ respectively for brevity. From [1, Prop. 1] and [2, Sec. 3.2],

$$R\mathcal{C}=(RG_C,Rc_C,A_C,b_C),\tag{4a}$$
$$\mathcal{C}\oplus\mathcal{S}=([G_C,G_S],c_C+c_S,[A_C,0;0,A_S],[b_C;b_S]),\tag{4b}$$
$$\begin{aligned}\mathcal{C}\cap_R\mathcal{W}=(&[G_C,0],c_C,[A_C,0;0,A_W;RG_C,-G_W],\\&[b_C;b_W;c_W-Rc_C]),\end{aligned}\tag{4c}$$
$$\begin{aligned}\mathcal{C}\cap\mathcal{H}=\Big(&[G_C,0],c_C,[A_C,0;p^\top G_C,d_m/2],\\&[b_C;(q+p^\top c_C-\|p^\top G_C\|_1)/2]\Big),\end{aligned}\tag{4d}$$

where $\mathcal{H}=\{x:p^\top x\leq q\}\subset\mathbb{R}^n$ is an halfspace, and (4d) also enables an exact computation of the intersection of a constrained zonotope and a polytope.

Recently, a least-squares-based approach was proposed to inner-approximate the Pontryagin difference between a full-dimensional constrained zonotope and a convex, compact, and symmetric set [5]. For the purposes of this paper, we recall the closed-form expression to inner-approximate $\mathcal{C}\ominus\mathcal{E}$, where $\mathcal{C}$ is a constrained zonotope and $\mathcal{E}$ is an ellipsoid.

Lemma 1. [5, Thm. 2, Corr. 1] *For a full-dimensional constrained zonotope $\mathcal{C}=(G_C,c_C,A_C,b_C)$ and an ellipsoid*

$$\mathcal{E}=(G_E,c_E)=\{G_E\gamma+c_E:\gamma\in\mathbb{R}^n,\|\gamma\|_2\leq 1\}\tag{5}$$

for some $G_E\in\mathbb{R}^{n\times n}$ and $c_E\in\mathbb{R}^n$, the constrained zonotope $\mathcal{M}^-$ satisfies

$$\mathcal{M}^-=(G_CD,c_C-c_E,A_CD,b_C)\subseteq\mathcal{C}\ominus\mathcal{E},\tag{6}$$

where $D=\mathrm{diag}_{i\in\mathbb{N}_{[1:N_C]}}(D_{ii})$ is a diagonal matrix with

$$D_{ii}=1-\left\|e_i^\top[G_C;A_C]^\dagger[G_E;0_{M_C\times n}]\right\|_2\geq 0.\tag{7}$$

Additionally, $\mathcal{M}^-=\mathcal{C}\ominus\mathcal{E}$, when $[G_C;A_C]$ is invertible.

Note that it is sufficient to consider symmetric $G_E\in\mathbb{S}_n$ in (5) [14, Ch. 8.4.2]. Additionally, for full-dimensional ellipsoids, it is sufficient to consider lower-triangular matrices $G_E\in\mathbb{L}_n$, where all diagonal entries of G_E are guaranteed to be non-zero [14, Ex. 3.27].

Lemma 1 along with (4) enable tractable computation of robust controllable sets of linear systems [5]. In Section V, we use these closed-form expressions to compute the terminal constraints on the rendezvous trajectory.

B. Problem statements

We now state the two problems of interest.

Problem 1. *Given a full-dimensional constrained zonotope $\mathcal{C}\subset\mathbb{R}^n$ and an ellipsoid $\mathcal{E}$ parameterized by (G_E,c_E),* *characterize a set of constraints that is sufficient to guarantee that $\mathcal{E} \subseteq \mathcal{C}$ and that is jointly convex in (G_E, c_E). Also, identify the additional requirements on $\mathcal{C}$ that makes these constraints necessary and sufficient.*

Problem 1 provides a set of sufficient conditions for tractable enforcement of chance constraints of the form $\mathbb{P}\{\boldsymbol{x} + z \in \mathcal{C}\} \geq \delta$. Additionally, Problem 1 also appears in the computation of maximum volume inscribed ellipsoid and Chebyshev centering for a constrained zonotope.

Problem 2. *Given a full-dimensional constrained zonotope $\mathcal{C} \subset \mathbb{R}^n$ and an ellipsoid $\mathcal{E}$, characterize a set of constraints that is both necessary and sufficient for $\mathcal{E} \cap \mathcal{C} = \emptyset$.*

Problem 2 provides a reformulation of chance constraints of the form $\mathbb{P}\{\boldsymbol{x} + z \notin \mathcal{C}\} \geq \delta$. However, unlike Problem 1, the set of constraints characterized for Problem 2 is bilinear in the parameters of the ellipsoid (G_E, c_E). These constraints may be enforced using solvers that can accommodate non-convex quadratic constraints [16].

III. Ellipsoid in a constrained zonotope

We now address Problem 1. We first characterize a set of constraints that is sufficient to guarantee $\mathcal{E} \subseteq \mathcal{C}$, and show that it is jointly convex in the parameters describing the ellipsoid. Then, we leverage these conditions on various applications in computational geometry and optimization problems with chance constraints.

A. Convex necessary and sufficient conditions for $\mathcal{E} \subseteq \mathcal{C}$

We use the definition of Pontryagin difference (3d) and Lemma 1 to address Problem 1.

Proposition 1. (Convex sufficient conditions) *For a full-dimensional constrained zonotope $\mathcal{C} = (G_C, c_C, A_C, b_C)$ (2b) and an ellipsoid $\mathcal{E} = (G_E, c_E)$ (5), $\mathcal{E} \subseteq \mathcal{C}$ if there exists $\xi \in \mathbb{R}^{N_C}, c \in \mathbb{R}^n, G_E \in \mathbb{S}_n$:*

$$G_C\xi + c_C = c_E \tag{8a}$$

$$A_C\xi = b_C \tag{8b}$$

$$|e_i^\top \xi| + \left\| e_i^\top [G_C; A_C]^\dagger [I_n; 0_{M_C \times n}] G_E \right\|_2 \leq 1, \tag{8c}$$

for all $i \in \mathbb{N}_{[1:N_C]}$. The set of constraints (8) is jointly convex in (ξ, G_E, c_E) for a given constrained zotonope $\mathcal{C}$.

Proof. For any set $\mathcal{C}, \mathcal{E} \subseteq \mathbb{R}^n$, $\mathcal{E} \subseteq \mathcal{C}$ if and only if $0 \in \mathcal{C} \ominus \mathcal{E}$ by (3d). Consequently, a sufficient condition for $\mathcal{E} \subseteq \mathcal{C}$ is that $0 \in \mathcal{M}^-$, for $\mathcal{M}^-$ defined in (6). Since $D_{ii} \geq 0$ (7) for all $i \in \mathbb{N}_{[1:N_C]}$,

$$\mathcal{M}^- = \left\{ G_C\xi + c_C - c_E \middle| A_C\xi = b_C, |e_i^\top \xi| \leq D_{ii} \right\} \tag{9}$$

from [5, Eq. (21) and (28)]. We complete the proof by observing that (8) follows from $0 \in \mathcal{M}^-$. □

Corollary 1. (Convex necessary and sufficient conditions for $\mathcal{E} \subseteq \mathcal{C}$) *For an ellipsoid $\mathcal{E}$ and a full-dimensional constrained zonotope $\mathcal{C}$ with an invertible matrix $[G_C; A_C]$, (8) is also necessary for $\mathcal{E} \subseteq \mathcal{C}$.*

Corollary 1 follows from the observation that $\mathcal{M}^- = \mathcal{M} = \mathcal{C} \ominus \mathcal{E}$ when $[G_C; A_C]$ is invertible (Lemma 1). Consequently, (8), which holds if and only if $0 \in \mathcal{M}^-$, is now necessary and sufficient for $\mathcal{E} \subseteq \mathcal{C}$.

Equation (8) imposes $(n + M_C)$ linear and N_C second order-cone constraints in $\xi \in \mathbb{R}^{N_C}$, $G_E \in \mathbb{S}_n$, and $c_E \in \mathbb{R}^n$.

B. Application in optimization with chance constraints: Probabilistic inclusion in a given constrained zonotope

Consider a decision variable $z \in \mathbb{R}^n$, a random vector $\boldsymbol{x} \sim \mathbb{P}$, and a constrained zonotope $\mathcal{C} \subset \mathbb{R}^n$. We seek to identify a set of constraints that is sufficient for

$$\mathbb{P}\{\boldsymbol{x} + z \in \mathcal{C}\} \geq \delta, \tag{10}$$

for some $\delta \in (0, 1)$. Chance constraints of the form (10) appears in model predictive control and motion planning problems under uncertainty [8], [12], [13], [17], where z may be the nominal state at a particular time instant, $\boldsymbol{x}$ may be the uncertainty and $\mathcal{C}$ may be the region of the state space that meets some safety specifications. We will use Proposition 1 and the well-known ellipsoidal approximation [12], [13] for chance constraints to arrive at a convex and deterministic sufficient conditions for (10).

We first recall a result based on the properties of Gaussian distribution and Chebyshev inequality [12], [13].

Lemma 2. (Ellipsoids containing δ-probability mass) *Given a n-dimensional random vector $\boldsymbol{x} \sim \mathbb{P}$ with mean $\mu_{\boldsymbol{x}} \in \mathbb{R}^n$ and a positive definite covariance $\Sigma_{\boldsymbol{x}} \in \mathbb{R}^{n \times n}$, and a probability threshold $\delta \in (0, 1)$. Then, $\mathbb{P}\{\boldsymbol{x} \in \mathcal{E}(\delta)\} \geq \delta$ for an ellipsoid,*

$$\mathcal{E}(\delta) = \left\{ K(\delta)\Sigma_{\boldsymbol{x}}^{\frac{1}{2}}\gamma + \mu_{\boldsymbol{x}} \middle| \gamma \in \mathbb{R}^n, \|\gamma\|_2 \leq 1 \right\}, \tag{11a}$$

$$K(\delta) = \begin{cases} \sqrt{\Phi^{-1}_{\chi^2(n)}(\delta)}, & \boldsymbol{x} \text{ is Gaussian}, \\ \sqrt{n/(1-\delta)}, & \text{otherwise}, \end{cases} \tag{11b}$$

where $\Phi^{-1}_{\chi^2(n)}$ is the inverse cumulative distribution function of the chi-square distribution with n degrees-of-freedom.

Proposition 2. (Ellipsoidal approximation of (10)) *Consider (10) where the random vector $\boldsymbol{x}$ has mean $\mu_{\boldsymbol{x}}$ and covariance $\Sigma_{\boldsymbol{x}}$, the constrained zonotope is $\mathcal{C} = (G_C, c_C, A_C, b_C)$ and the threshold is $\delta \in (0, 1)$. Then, (10) holds if there exists $(z, \xi) \in \mathbb{R}^n \times \mathbb{R}^{N_C}$ that satisfies,*

$$G_C\xi + c_C - (\mu_{\boldsymbol{x}} + z) = 0, \tag{12a}$$

$$A_C\xi = b_C, \tag{12b}$$

$$|e_i^\top \xi| + K(\delta) \left\| e_i^\top [G_C; A_C]^\dagger [I_n; 0_{M_C \times n}] \Sigma_{\boldsymbol{x}}^{\frac{1}{2}} \right\|_2 \leq 1. \tag{12c}$$

Proof. By Proposition 1, (12) enforces $\{\boldsymbol{x} + z \in \mathcal{E}(\delta)\} \subseteq \{\boldsymbol{x} + z \in \mathcal{C}\}$ for any $z \in \mathbb{R}^n$. Consequently, $\mathbb{P}\{\boldsymbol{x} + z \in \mathcal{C}\} \geq \mathbb{P}\{\boldsymbol{x} + z \in \mathcal{E}(\delta)\} \geq \delta$ by (1b) and Lemma 2. □

Constraints (12) are linear in the decision variables z and ξ. The choice of K in (12c) depends on whether $\boldsymbol{x}$ is Gaussian or non-Gaussian (11b). We refer to Proposition 2 as the *ellipsoidal approximation* of (10) [12].

With Proposition 2, we obtain a tractable approximation of stochastic programs of the form,

$$\underset{z\in\mathcal{Z}}{\text{maximize}} \quad \mathbb{P}\{\boldsymbol{x}+z\in\mathcal{C}\}. \tag{13}$$

for some convex set $\mathcal{Z}\subseteq\mathbb{R}^n$. Using the observation that K is monotonic in δ [14, Ch. 4.2.4], consider the deterministic approximation of (13),

$$\begin{array}{rl} \text{max.} & k \\ \text{s. t.} & z\in\mathcal{Z}, k\geq 0, \xi\in\mathbb{R}^{N_C}, \\ & G_C\xi + c_C = \mu,\ \ A_C\xi = b_C, \\ i\in\mathbb{N}_{[1:N_C]}, & |e_i^\top\xi| + k\|e_i^\top[G_C;A_C]^\dagger[I_n;0_{M_C\times n}]\Sigma_{\boldsymbol{x}}\|_2\leq 1, \end{array} \tag{14}$$

with decision variables z, k, and ξ. Problem (14) is a convex program, and is linear when $\mathcal{Z}$ is a polytope. By Proposition 2, the optimal solution of (14), denoted by $(z^\dagger, k^\dagger, \xi^\dagger)$, is a feasible (but possibly suboptimal) solution to (13). Specifically, denoting the optimal solution of (13) by z^*,

$$\mathbb{P}\{\boldsymbol{x}+z^*\in\mathcal{C}\}\geq\mathbb{P}\{\boldsymbol{x}+z^\dagger\in\mathcal{C}\}\geq K^{-1}(k^\dagger).$$

C. Application in computational geometry: Maximum volume inscribed ellipsoid and Chebyshev centering

We apply Proposition 1 to two computational geometry problems — approximating the maximum volume inscribed ellipsoid and Chebyshev center of a constrained zonotope.

1) Maximum volume inscribed ellipsoid: Given a full-dimensional constrained zonotope $\mathcal{C}$, we seek the maximum volume inscribed ellipsoid $\mathcal{E}=(G_E,c_E)\subseteq\mathcal{C}$.

Since the maximum volume inscribed ellipsoid of a full-dimensional constrained zonotope is also full-dimensional, we consider $G_E\in\mathbb{L}_n$. Additionally, the volume of such an ellipsoid is proportional to $\left(\prod_{i=1}^n G_{E,ii}\right)^{\frac{1}{n}}$, the geometric mean of the diagonal entries of G_E [14, Ex. 3.26].

Consider the following optimization program,

$$\begin{array}{rl} \text{max.} & \left(\prod_{i=1}^n G_{E,ii}\right)^{\frac{1}{n}} \\ \text{s. t.} & \xi\in\mathbb{R}^{N_C},\ G_E\in\mathbb{L}_n,\ c_E\in\mathbb{R}^n \\ & G_C\xi + c_C = c_E,\ \ A_C\xi = b_C, \\ i\in\mathbb{N}_{[1:N_C]}, & |e_i^\top\xi| + \left\|e_i^\top[G_C;A_C]^\dagger[I_n;0_{M_C\times n}]G_E\right\|_2\leq 1. \end{array} \tag{15}$$

Problem (15) is a second-order cone program, since the objective may be imposed as a second-order cone constraint [14, Ex. 4.26], and the constraints are linear or second-order cone constraints in ξ, G_E, and c_E.

2) Chebyshev centering: The Chebyshev centering may be viewed as a special case of the maximum volume inscribed ellipsoid, where we optimize for the maximum volume inscribed *sphere* [14, Ch. 8.5.1]. Consequently, by substituting $G_E = RI_n$ in (15) for some $R>0$, the following linear optimization program,

$$\begin{array}{rl} \text{max.} & R \\ \text{s. t.} & \xi\in\mathbb{R}^{N_C},\ R>0,\ c_E\in\mathbb{R}^n \\ & G_C\xi + c_C = c_E,\ \ A_C\xi = b_C, \\ i\in\mathbb{N}_{[1:N_C]}, & |e_i^\top\xi| + R\left\|e_i^\top[G_C;A_C]^\dagger[I_n;0_{M_C\times n}]\right\|_2\leq 1, \end{array} \tag{16}$$

computes an approximate Chebyshev center c_E^* of the constrained zonotope $\mathcal{C}$.

Problems (15) and (16) may yield an inscribed ellipsoid or a sphere that is suboptimal in volume due to their use of sufficient conditions to enforce $\mathcal{E}\subseteq\mathcal{C}$ (Proposition 1). However, (15) and (16) recover the true maximum volume inscribed ellipsoid and the Chebyshev center when $[G_C;A_C]$ is invertible (Corollary 1).

D. Discussion

The constraints in (8), (12), (14), (15) and (16) in their current form require the computation of the pseudoinverse $[G_C;A_C]^\dagger$, which can be computationally expensive for large N_C and M_C. On the other hand, $\Gamma=[G_C;A_C]^\dagger[I_n;0_{M_C\times n}]$ may also be computed directly without an explicit computation of psuedoinverse via QR factorization or complete orthogonal decomposition (see [5, Sec. 4.4] for more details). We utilized `lsqminnorm` to compute Γ [5], [18].

IV. Ellipsoid outside a constrained zonotope

We now turn our attention to Problem 2. Given an ellipsoid $\mathcal{E}$ and a constrained zonotope $\mathcal{C}$, we propose a set of constraints that is both necessary and sufficient to guarantee that $\mathcal{E}\cap\mathcal{C}=\emptyset$, and use them to enforce $\mathbb{P}\{\boldsymbol{x}+z\notin\mathcal{C}\}\geq\delta$.

A. Necessary and sufficient conditions for $\mathcal{C}\cap\mathcal{E}=\emptyset$

We address Problem 2 using strong duality and separating hyperplane theorem.

Proposition 3. (Necessary and sufficient conditions for $\mathcal{E}\cap\mathcal{C}=\emptyset$) *For a full-dimensional constrained zonotope $\mathcal{C}=(G_C,c_C,A_C,b_C)$ (2b) and an ellipsoid $\mathcal{E}=(G_E,c_E)$ (5) with $G_E\in\mathbb{L}_n$, $\mathcal{C}\cap\mathcal{E}=\emptyset$ if and only if there exists $\ell\in\mathbb{R}^n, \nu\in\mathbb{R}^{M_C}$ such that*

$$\|\ell\|_2\leq 1 \tag{17a}$$

$$\ell^\top(c_E-c_C)+\nu^\top b_C+\|G_E^\top\ell\|_2+\left\|G_C^\top\ell+A_C^\top\nu\right\|_1<0. \tag{17b}$$

Proof. Recall that a necessary and sufficient condition for $\mathcal{E}\cap\mathcal{C}=\emptyset$ is that there exists $\ell\in\mathbb{R}^n$,

$$\sup_{x\in\mathcal{E}}\ell^\top x<\inf_{x\in\mathcal{C}}\ell^\top x. \tag{18}$$

with $\|\ell\|_2\leq 1$ [14, Sec. 8.2.3]. The LHS of (18) is the support function of an ellipsoid, which is known in closed form $\sup_{x\in\mathcal{E}}\ell^\top x=\ell^\top c_E+\|G_E^\top\ell\|_2$. For a full-dimensional constrained zonotope, we use strong duality [14, Sec. 5.2.3] to express the RHS of (18), $\inf_{x\in\mathcal{C}}\ell^\top x=\sup_{\nu\in\mathbb{R}^{M_C}}\left(-\nu^\top b+\ell^\top c_C-\left\|G_C^\top\ell+A_C^\top\nu\right\|_1\right)$. We obtain (17) by combining these observations. □

Constraints (17) are second-order cone constraints in ℓ and ν, and hence convex. However, unlike Proposition 1, these constraints are non-convex in the parameters (G_E,c_E).

B. Application in optimization with chance constraints: Probabilistic exclusion from a given constrained zonotope

Consider a decision variable $z\in\mathbb{R}^n$, a random vector $\boldsymbol{x}\sim\mathbb{P}$, and a constrained zonotope $\mathcal{C}\subset\mathbb{R}^n$. We seek a set of constraints that is necessary and sufficient for

$$\mathbb{P}\{\boldsymbol{x}+z\notin\mathcal{C}\}\geq\delta, \tag{19}$$

for some $\delta \in (0,1)$. Chance constraints of the form (19) appears in model predictive control and motion planning problems [13] under uncertainty, where $\mathcal{C}$ may be a region of the state space that do not meet some safety specifications. Using Proposition 3, we can characterize a set of deterministic constraints that is necessary and sufficient for (19).

Proposition 4. (ELLIPSOIDAL APPROXIMATION OF (19)) *Consider a random vector $\boldsymbol{x}$ with mean $\mu_{\boldsymbol{x}}$ and covariance $\Sigma_{\boldsymbol{x}}$, the constrained zonotope is $\mathcal{C} = (G_C, c_C, A_C, b_C)$ and the threshold is $\delta \in (0,1)$. Then,* (19) *holds if and only if there exists $(z,\ell,\nu) \in \mathbb{R}^n \times \mathbb{R}^n \times \mathbb{R}^{M_C}$ that satisfy,*

$$\begin{aligned} \|\ell\|_2 &\leq 1 \\ \ell^\top (z + c_E - c_C) + \nu^\top b_C + K(\delta)\|\Sigma_{\boldsymbol{x}}^{\frac{1}{2}}\ell\|_2 + \|G_C^\top \ell + A_C^\top \nu\|_1 &< 0. \end{aligned} \tag{20}$$

Proof. Proof. It is sufficient to show that $\mathbb{P}\{\boldsymbol{x} + z \in \mathcal{C}\} \leq 1-\delta$. By Proposition 3, (20) enforces $(z + \mathcal{E}(\delta)) \cap \mathcal{C} = \emptyset$, which implies that $\mathcal{C} \subseteq \mathbb{R}^n \setminus (z + \mathcal{E}(\delta))$. From (1b) and Lemma 2, $\mathbb{P}\{\boldsymbol{x} + z \in \mathcal{C}\} \leq \mathbb{P}\{\boldsymbol{x} + z \in \mathbb{R}^n \setminus (z + \mathcal{E}(\delta))\} = \mathbb{P}\{\boldsymbol{x} \notin \mathcal{E}(\delta)\} \leq 1-\delta$, as desired. ☐

Unlike Proposition 2, Proposition 4 is non-convex in the optimization variables z, ℓ, and ν, due to the bilinearity $\ell^\top z$ in (20). One could either use solvers that accommodate non-convex quadratic constraints [16] to tackle the bilinearity exactly or enforce (20) conservatively by fixing ℓ.

V. RETURN-GUARANTEED SPACECRAFT RENDEZVOUS

We consider the problem of a two-staged spacecraft rendezvous. For the first stage, we design a rendezvous trajectory for an approaching spacecraft (deputy) navigate towards another spacecraft (chief), while minimizing fuel usage and maintaining it inside a line-of-sight cone [6], [8]. The rendezvous trajectory must also be cognizant of the process noise arising from the actuator limitations of the spacecraft and the navigational uncertainty arising from sensing limitations [6]. The rendezvous trajectory of the first phase terminates with the deputy at a hold position near the chief, and the deputy waiting for a go/no-go decision.

During the second stage, the deputy must meet two mission requirements depending on the go/no-go decision issued by the chief. If a go decision is issued, the deputy proceeds to rendezvous with the chief. On the other hand, if a no-go decision is issued, the deputy must return to a pre-determined holding position further away from the chief. Retaining the ability to return to the holding position can be beneficial when the deputy terminates the first phase at an unanticipated configuration possibly due to uncertainty.

While a rendezvous trajectory may be synthesized for both stages of these missions simultaneously, such a design process can be computationally expensive, and may become difficult with increasing mission complexity/stages. Instead, we simplify the rendezvous trajectory design by encoding the mission requirements of the subsequent stages as terminal constraints on the first stage using reachability, specifically robust controllable sets similarly to [5], [7], [8]. Due to high-dimensionality and long horizons, polytope-based computations of controllable sets face challenges, while we found constrained zonotopes to be significantly more stable with minor conservativeness [5].

Dynamics: The relative dynamics between the spacecraft are described by the Hill-Clohessy-Wiltshire (HCW) equations [6] with additive stochastic noise,

$$\ddot{p_x} - 3\omega p_x - 2\omega \dot{p_y} = m_d^{-1} F_x, \qquad \ddot{p_y} + 2\omega \dot{p_x} = m_d^{-1} F_y. \tag{21}$$

The chief is located at the origin, the position of the deputy is $p_x, p_y \in \mathbb{R}$, $\omega = \sqrt{\mu / R_0^3}$ is the orbital frequency, μ is the gravitational constant, and R_0 is the orbital radius of the spacecraft. See [8] for further details and numerical values.

We define the state as $x = [p_x, p_y, v_x, v_y] \in \mathbb{R}^4$ (relative position and velocity) and the input as $u = [F_x, F_y] \in \mathcal{U} \subseteq \mathbb{R}^2$. We discretize (21) using a zero-order hold at sampling time of 30 seconds to obtain,

$$\boldsymbol{x}_{t+1} = A\boldsymbol{x}_t + B(u_t + \boldsymbol{w}_t), \quad \boldsymbol{y}_{t+1} = \boldsymbol{x}_{t+1} + \boldsymbol{\eta}_{t+1} \tag{22}$$

with state measurement $\boldsymbol{y}_k \in \mathbb{R}^4$, input space $\mathcal{U} = [-5,5]^2$ N, and Gaussian disturbances $\boldsymbol{w}_k \in \mathbb{R}^2$ and $\boldsymbol{\eta}_k \in \mathbb{R}^4$ with zero means and covariance matrices $\Sigma_{\boldsymbol{w}} = 0.0003 I_2$ and $\Sigma_{\boldsymbol{\eta}} = 0.0003 \times \mathrm{diag}([1,1,0,0])$ respectively. Due to Gaussian disturbances $\boldsymbol{w}$ and $\boldsymbol{\eta}$, $\boldsymbol{x}$ and $\boldsymbol{y}$ are also Gaussian.

Second-phase mission requirements: We define the following sets (positions and velocities measured in m and m/s),

$$\begin{aligned} \mathcal{T} &= \left\{x \in \mathbb{R}^4 : |p_x| \leq 200, |p_y| \leq 200, |v_x| \leq 0.1, |v_y| \leq 0.1\right\}, \\ \mathcal{H}_0 &= \left\{x \in \mathbb{R}^4 : |p_x| \leq 10, |p_y| \leq 50, |v_x| \leq 0.05, |v_y| \leq 0.05\right\}, \\ \mathcal{S} &= \left\{x \in \mathbb{R}^4 : |p_x| \leq -p_y \leq 2000, |v_x| \leq 0.5, |v_y| \leq 0.5\right\}, \end{aligned}$$

where $\mathcal{T}$ is the target set that the deputy must reach in the event of go, $\mathcal{H} \triangleq [0; -1600; 0; 0] + \mathcal{H}_0$ is the pre-determined holding position that the deputy must return to in the event of no-go, and $\mathcal{S}$ is the line-of-sight cone.

We assume the planning horizons for the first and second stages are $T_1, T_2 \in \mathbb{N}$ respectively. We chose $T_1 = 0.75$ hours and $T_2 = 0.5$ hours (90 and 60 time steps respectively). We also define two sequences of sets $\mathscr{S}_{\text{go}}$ and $\mathscr{S}_{\text{no-go}}$ to encode the different mission objectives in the second-stage:

$$\mathscr{S}_{\text{go}} = \{\underbrace{\mathcal{S}, \ldots, \mathcal{S}}_{T_2 - 1}, \mathcal{T}\} \subseteq (\mathbb{R}^n)^{T_2}, \tag{23a}$$

$$\mathscr{S}_{\text{no-go}} = \{\underbrace{\mathcal{S}, \ldots, \mathcal{S}}_{T_2 - 1}, \mathcal{H}\} \subseteq (\mathbb{R}^n)^{T_2}. \tag{23b}$$

Denoting the terminal state measurement at the end of first-phase by $\boldsymbol{y}_{T_1}$, we encode the second-phase mission requirements as follows,

$$\mathbb{P}\left\{\boldsymbol{y}_{T_1} \in \mathcal{L}^{\text{meas}}(\alpha_{\text{no-go}}, \mathscr{S}_{\text{no-go}})\right\} \geq \delta_{\text{no-go}}, \tag{24a}$$

$$\mathbb{P}\left\{\boldsymbol{y}_{T_1} \in \mathcal{L}^{\text{meas}}(\alpha_{\text{go}}, \mathscr{S}_{\text{go}})\right\} \geq \delta_{\text{go}}, \tag{24b}$$

where, $\mathcal{L}^{\text{meas}}(\alpha, \mathscr{S})$ is the α-stochastic reachable set,

$$\mathcal{L}^{\text{meas}}(\alpha, \mathscr{S}) = \left\{ y_0 \;\middle|\; \begin{array}{c} \exists \pi \in \mathscr{U}, \\ \mathbb{P}_{\boldsymbol{x}}^{\pi, y_0}\{\forall t \in \mathbb{N}_{[1:T]},\ \boldsymbol{x}_t \in \mathcal{S}_t\} \geq \alpha \end{array} \right\}. \tag{25}$$

Here, $\mathscr{U}$ is the set *measurement-feedback policies* $\pi = \{\pi_t\}_t$ with $\pi_t : \mathbb{R}^n \to \mathcal{U}$ as a *measurement-feedback controller* that maps the current state measurement $y \in \mathbb{R}^n$ to a feasible input $\pi(y) \in \mathcal{U}$. Additionally in (25), $\mathbb{P}^{\pi,y_0}_{\boldsymbol{x}}$ denotes the probability measure of the stochastic process $\{\boldsymbol{x}\}_{t=0}^{T}$, based on the dynamics (22) and the probability measures $\mathbb{P}_{\boldsymbol{\eta}}, \mathbb{P}_{\boldsymbol{w}}$. Moving back to (24), $\alpha_{\text{go}}, \alpha_{\text{no-go}}, \delta_{\text{go}}, \delta_{\text{no-go}} \in (0,1)$ with α_{go} and $\alpha_{\text{no-go}}$ as the desired likelihoods of successful rendezvous with $\mathcal{T}$ or return to $\mathcal{H}$ in the second phase respectively, and δ_{go} and $\delta_{\text{no-go}}$ as the desired likelihoods of the first phase terminating with a state measurement $\boldsymbol{y}_{T_1}$ that allows for completing the second phase's go and no-go mission objectives respectively. Unless specified otherwise, we chose $\delta_{\text{go}} = \delta_{\text{no-go}} = \alpha_{\text{go}} = \alpha_{\text{no-go}} = 0.9$.

The constraint (24) eliminates the need to design the second phase's trajectory during the first phase. However, an exact computation of $\mathcal{L}^{\text{meas}}$ is hard and may require dynamic programming [17]. Therefore, we use robust controllable sets to inner-approximate $\mathcal{L}^{\text{meas}}$, similarly to [8, Thm. 1].

Proposition 5. *Given a threshold* $\alpha \in (0,1)$*, choose* $\alpha_\eta, \alpha_w \in (0,1)$ *with* $\alpha_\eta^{(T+1)}\alpha_w^{(T)} \geq \alpha$*. Define* $\mathcal{E}_\eta \subset \mathbb{R}^n$ *and* $\mathcal{E}_w \subset \mathbb{R}^p$ *such that*

$$\mathbb{P}_{\boldsymbol{\eta}}\{\boldsymbol{\eta} \in \mathcal{E}_\eta\} \geq \alpha_\eta, \text{ and } \mathbb{P}_{\boldsymbol{w}}\{\boldsymbol{w} \in \mathcal{E}_w\} \geq \alpha_w. \tag{26}$$

Define $\mathcal{E}_\phi \triangleq (F\mathcal{E}_w) \oplus (-A\mathcal{E}_\eta) \oplus (-\mathcal{E}_\eta)$*. Then,* $\mathcal{K}^{\text{meas}}(\alpha, \mathscr{S}) \triangleq \mathcal{K}_0 \subseteq \mathcal{L}^{\text{meas}}(\alpha, \mathscr{S})$*, where* $\mathcal{K}_0$ *is given by the following set recursion (with* $\mathcal{K}_T \triangleq \mathcal{S}_T$*),*

$$\mathcal{K}_t = \text{Pre}(\mathcal{K}_{t+1} \ominus (-\mathcal{E}_\eta)) \cap \mathcal{S}_t, \quad \forall t \in \mathbb{N}_{[0:T-1]}, \tag{27a}$$

$$\text{Pre}(\mathcal{K}_{t+1}) \triangleq \{x : A_t x \in (\mathcal{K}_{t+1} \ominus \mathcal{E}_\phi) \oplus (-B_t\mathcal{U})\}. \tag{27b}$$

We tractably enforce (24) using Propositions 5 and 2 and constrained zonotopes $\mathcal{K}^{\text{meas}}(\alpha, \mathscr{S})$ [5].

First-phase mission requirements: We consider two types of stochastic optimal control problems for the rendezvous trajectory design in the first phase.

Guidance problem 1: Minimum final distance

$$\underset{\substack{u_0,\ldots,u_{T_1-1},\\ \xi_{\text{go}},\xi_{\text{no-go}}}}{\text{minimize}} \quad \|e_2^\top \mathbb{E}[\boldsymbol{x}_{T_1}]\|_2^2 + \lambda \sum_{t=0}^{T_1-1} \|u_t\|_2 \tag{28a}$$

$$\text{subject to} \quad e_2^\top \mathbb{E}[\boldsymbol{x}_{T_1}] \leq D, \mathbb{E}[\boldsymbol{x}_{j,T_1}] = 0, \forall j \in \{1,3,4\}, \tag{28b}$$

$$t \in \mathbb{N}_{[0:T_1-1]}, \quad u_t \in \mathcal{U},\ \mathbb{P}\{\boldsymbol{x}_{t+1} \in \mathcal{S}\} \geq \delta_{\text{LoS}},, \tag{28c}$$

$$\text{Dynamics (22) from initial measurement } y_0 \tag{28d}$$

$$\text{(24) using (12) with } \xi_{\text{go}}, \xi_{\text{no-go}}. \tag{28e}$$

Guidance problem 2: Maximize second-phase success

$$\underset{\substack{u_0,\ldots,u_{T_1-1},\\ k_{\text{go}},k_{\text{no-go}},\xi_{\text{go}},\xi_{\text{no-go}}}}{\text{maximize}} \quad k_{\text{go}} \tag{29a}$$

$$\text{subject to} \quad \text{(28b)–(28d)},$$

$$\sum\nolimits_{t=0}^{T_1-1} \|u_t\|_2 \leq \Delta v_{\max} \tag{29b}$$

$$\text{(24) using (14) with } k_{\text{go}}, k_{\text{no-go}}, \xi_{\text{go}}, \xi_{\text{no-go}}. \tag{29c}$$

$$k_{\text{go}} \geq K(\delta_{\text{go}}), k_{\text{no-go}} \geq K(\delta_{\text{no-go}}) \tag{29d}$$

Recall that $[p_x, v_x, v_y] = [0,0,0]$ is an equilibrium point for the HCW dynamics (21) irrespective of p_y [6]. In the first guidance problem (28), constraint (28b) allows the deputy to wait for the go/no-go decision at the end of the first phase at a relative distance from the chief not larger than $D > 0$. Thus, objective (28a) together with (28b) requires the deputy to terminate the first phase close to the target set $\mathcal{T}$ in expectation, while minimizing the net fuel cost incurred during the maneuver. The net energy consumed by the manuever as it appears in (28a) is also denoted by Δv,

$$\Delta v = \sum\nolimits_{t=0}^{T_1-1} \|u_t\|_2. \tag{30}$$

The weight $\lambda > 0$ prescribes the relative importance of the two objectives of the first-phase. Constraint (28c) encodes the control constraints and the chance constraints associated with the line-of-sight cone. Constraint (28d) imposes the physical constraints on the spacecraft arising the dynamics (22), and constraint (28e) enforces the terminal chance constraints (24). We chose $D = 500$ m, and $\lambda = 10$.

In the second guidance problem (29), we impose almost all of the constraints of (28), but now seek to maximize $\mathbb{P}\left\{\boldsymbol{y}_{T_1} \in \mathcal{L}^{\text{meas}}(\alpha_{\text{go}}, \mathscr{S}_{\text{go}})\right\}$ using the formulation in (14). We additionally impose an upper-bound on the incurred net energy $\sum_{t=0}^{T_1-1} \|u_t\|_2$ by $\Delta v_{\max}$. We chose $\Delta v_{\max} = 10$ m/s.

We performed the presented computations in a standard computer with Intel CPU i9-12900KF processor (3.2 GHz, 16 cores) and 64 GB RAM, running MATLAB 2022b. We used `SReachTools` [19], `YALMIP` [20], `MPT3` [21], and `MOSEK` [22] to formulate and solve the stochastic optimal problems. After solving (28) and 29, we generated 10^5 samples of $\{\boldsymbol{x}_t\}_{t=1}^{T}$ and $\boldsymbol{y}_{T_1}$ to check satisfaction of (24). We also took 100 samples of $\boldsymbol{y}_{T_1}$ and simulated the success probability of the second phase after computing their corresponding π_{robust}. Since a naive Monte-Carlo simulation is challenging due to the high-branching factor, we used an "adversarial" realization of the disturbances at each time step, where we selected the sample that pushes the trajectory furthest away from the intended target the most.

Table I summarizes various metrics associated with each problem. The computation of terminal state constraints $\mathcal{K}^{\text{meas}} \subseteq \mathcal{L}^{\text{meas}}$ as constrained zonotopes for both objectives of the second phase took about 1 minute, despite a relatively long horizon $T_2 = 60$ steps. In contrast, we were unable to compute $\mathcal{K}^{\text{meas}}$ for either of the objectives using polyhedral computations (`MPT3`) due to numerical issues from vertex-facet enumeration [21]. The solve times for (28) and (29) were comparable.

Table I also shows that the safety and the performance of the rendezvous maneuver generated (28) and (29) are different due to the different formulations. Problem (28) computes a rendezvous manuever for the deputy that meets all the mission requirements of the first and second stages. On the other hand, Problem (29) computes a rendezvous manuever for the deputy with higher docking probability (0.99 vs 0.94), while resulting in a relatively further terminal position (922.85 m vs 786.80 m) and higher Δv (6.57

TABLE I

VARIOUS METRICS OF PERFORMANCE AND SAFETY FOR THE TWO-STAGED SPACECRAFT RENDEZVOUS PROBLEM.

Problem	Compute time (in seconds)			Δv	$\mathrm{dist}(\mathbb{E}[\boldsymbol{x}_T], \mathcal{T})$	$\mathbb{P}\{\boldsymbol{x}_t \in \mathcal{S}\}$		No-go mission (return) prob. (24a)		Go mission (dock) prob. (24b)	
	$\mathcal{K}^{\mathrm{meas}}_{\text{no-go}}$	$\mathcal{K}^{\mathrm{meas}}_{\text{go}}$	Solve time	(in m/s)	(in m.)	δ_{LoS}	Monte-Carlo est.	$(\delta_{\text{no-go}}, \alpha_{\text{no-go}})$	Monte-Carlo est.	$(\delta_{\text{go}}, \alpha_{\text{go}})$	Monte-Carlo est.
Min. distance (28)	0.56	0.49	0.33	5.61	786.80	0.90	1.00	(0.90, 0.90)	(1.00, 1.00)	(0.90, 0.90)	(0.94, 0.97)
Max. success (29)			0.27	6.57	922.85	0.90	1.00	(0.95*, 0.90)	(1.00, 1.00)	(0.91*, 0.90)	(0.99, 1.00)

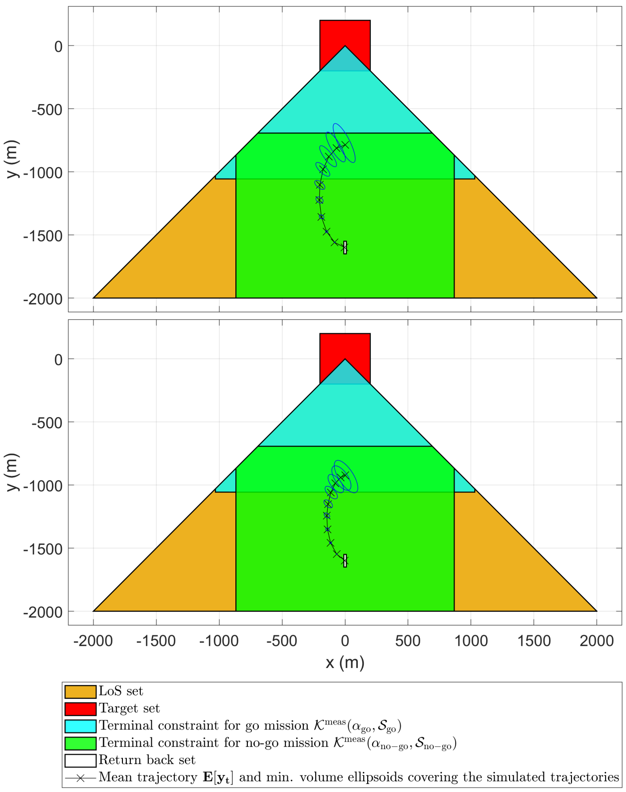

Fig. 1. Rendezvous trajectories using the different guidance problems (28) (top) and (29) (bottom), along with the projection of the four-dimensional terminal constraint sets $\mathcal{K}^{\mathrm{meas}}$ on to the x-y plane. The sets $\mathcal{K}^{\mathrm{meas}}$ are computed using Proposition 5 and constrained zonotopes.

m/s vs 5.61 m/s). The conservativeness introduced by the Proposition 2 is evident with the Monte-Carlo simulations reporting much higher degree of safety than the required δ.

Figure 1 shows the rendezvous trajectory computed using (28) and (29) as well as constrained zonotope sets $\mathcal{K}^{\mathrm{meas}}$ that inner-approximate $\mathcal{L}^{\mathrm{meas}}$ in (24). As seen from Table I as well, the rendezvous trajectory from (28) brings the deputy closer to the chief as compared to the rendezvous trajectory from (29). The ellipsoids in Figure 1 are the minimum volume ellipsoids that contain the spread of the Monte-Carlo simulation trajectories around the mean trajectory (see [14, Sec. 8.4.1] for the computation of the ellipsoids).

VI. CONCLUSION

We considered the problems of inscribing an ellipsoid within and separating an ellipsoid from a constrained zonotope. We proposed a set of sufficient conditions that are convex in the parameters and guarantee that an ellipsoid is inscribed within a constrained zonotope, and a set of necessary and sufficient conditions that are non-convex in the parameters to separate an ellipsoid from a constrained zonotope. We applied these constraints to tractably solve a two-stage return-guaranteed spacecraft rendezvous problem, and also tractably approximate the Chebyshev center and the maximum volume inscribed ellipsoid of a constrained zonotope using linear and second-order cone programming.

REFERENCES

[1] J. Scott, D. Raimondo, G. Marseglia, and R. Braatz, "Constrained zonotopes: A new tool for set-based estimation and fault detection," *Automatica*, vol. 69, pp. 126–136, 2016.

[2] V. Raghuraman and J. Koeln, "Set operations and order reductions for constrained zonotopes," *Automatica*, vol. 139, 2022.

[3] L. Yang, H. Zhang, J. Jeannin, and N. Ozay, "Efficient backward reachability using the Minkowski difference of constrained zonotopes," *IEEE Trans. Comp.-Aided Design Integ. Circ. Syst.*, vol. 41, no. 11, pp. 3969–3980, 2022.

[4] M. Althoff, "An introduction to CORA," in *Proc. App. Verif. Cont. Hybrid Syst.*, December 2015, pp. 120–151.

[5] A. Vinod, A. Weiss, and S. D. Cairano, "Projection-free computation of robust controllable sets with constrained zonotopes," 2024, https://arxiv.org/abs/2403.13730 (Available online).

[6] W. Fehse, *Automated rendezvous and docking of spacecraft*. Cambridge Univ. Press, 2003, vol. 16.

[7] D. Marsillach, S. Di Cairano, and A. Weiss, "Abort-safe spacecraft rendezvous on elliptic orbits," *IEEE. Trans. Ctrl. Syst. Tech.*, vol. 31, pp. 1133 – 1148, 2022.

[8] A. Vinod, A. Weiss, and S. Di Cairano, "Abort-safe spacecraft rendezvous under stochastic actuation and navigation uncertainty," in *Proc. Conf. Dec. & Ctrl.*, 2021, pp. 6620–6625.

[9] F. Blanchini and S. Miani, *Set-theoretic analysis of dynamic systems*. Springer International Publishing, 2015.

[10] C. Jones, E. Kerrigan, and J. Maciejowski, "On polyhedral projection and parametric programming," *J. Opt. Theory App.*, vol. 138, pp. 207–220, 2008.

[11] F. Borrelli, A. Bemporad, and M. Morari, *Predictive control for linear and hybrid systems*. Cambridge Univ. Press, 2017.

[12] D. Van Hessem and O. Bosgra, "Stochastic closed-loop model predictive control of continuous nonlinear chemical processes," *Journal of Process Control*, vol. 16, no. 3, pp. 225–241, 2006.

[13] T. Lew, R. Bonalli, and M. Pavone, "Chance-constrained sequential convex programming for robust trajectory optimization," in *Proc. Euro. Ctrl. Conf.*, 2020, pp. 1871–1878.

[14] S. Boyd and L. Vandenberghe, *Convex optimization*. Cambridge Univ. Press, 2004.

[15] X. Zhang, A. Liniger, and F. Borrelli, "Optimization-based collision avoidance," *IEEE. Trans. Ctrl. Syst. Tech.*, vol. 29, pp. 972–983, 2020.

[16] Gurobi Opt., LLC, "Gurobi Optimizer Reference Manual," https://www.gurobi.com (Last accessed: 2023).

[17] J. Gleason, A. Vinod, and M. Oishi, "Lagrangian approximations for stochastic reachability of a target tube," *Automatica*, vol. 125, 2021.

[18] MathWorks, "`lsqminnorm`: Minimum norm least-squares solution to linear equation," https://mathworks.com/help/matlab/ref/lsqminnorm.html.

[19] A. Vinod, J. Gleason, and M. Oishi, "SReachTools: a MATLAB stochastic reachability toolbox," in *Proc. Hybrid Syst.: Comp. & Ctrl.*, 2019, pp. 33–38.

[20] J. Lofberg, "YALMIP: A toolbox for modeling and optimization in MATLAB," in *IEEE Intn'l Conf. Rob. Autom.*, 2004, pp. 284–289.

[21] M. Herceg, M. Kvasnica, C. Jones, and M. Morari, "Multi-Parametric Toolbox 3.0," in *Proc. Euro. Ctrl. Conf.*, 2013, pp. 502–510.

[22] MOSEK, *The MOSEK optimization toolbox for MATLAB manual. Version 10.0.*, 2022. [Online]. Available: http://docs.mosek.com/10.0/toolbox/index.html